A study of growth and breakdown of passive film on copper surface by electrochemical impedance spectroscopy

Amtul NASEER[*] **and Athar Yaseen KHAN**

Department of Chemistry, Quaid- i-Azam University, Islamabad-PAKISTAN
e-mail: hanm_7@yahoo.com

Electrochemical impedance spectroscopy (EIS) and cyclic voltammetry were used to investigate the oxide layer formed on a copper disc electrode and the changes that took place when treated potentiostatically in the range of -0.3 V to 0.9 V in aqueous buffer solution of pH 9.2. Equivalent circuits were used to model the response of the electrode, initially at equilibrium to an applied potential. These circuits were proposed for different potential ranges in order to illustrate the Cu/oxide/electrolyte system and its properties in terms of 2 interfaces. A criterion for the applicability of equivalent circuit models was discussed. Changes in the film/metal interface as a function of potential were probed at 30 mHz from Nyquist plots. Diffusion coefficient calculated for the ionic movement in the film at 2 potential values using EIS data was of the order of 10^{-9} cm^2 s^{-1}.

Key Words: Copper, electrochemical impedance spectroscopy, cyclic voltammetry, passive film, interfaces.

Introduction

Corrosion of copper occurs in presence of oxygen when in contact with electrolytes.[1] Thin film formed over copper in anodic conditions in neutral,[2] weakly acidic, or alkaline aqueous[3] media has attracted considerable interest of researchers studying corrosion, electro catalysis, and double layer structures.[4] Passive layers on copper metal have been widely investigated[5−8] and several surface analytical and electrochemical tools have been used.[9−13] Some of the obvious factors affecting the thickness and structure of the oxide film are pH, potential, and the time of contact with the aqueous environment.

---

[*]Corresponding author

Electrochemical impedance spectroscopy is a powerful and sensitive in situ technique to characterize surfaces. Its potential in the study of corrosion of copper[3,14−16]has not been fully realized. Metals exhibit inhomogeneous surfaces obstructing corrosion studies. However, even though inclusion of a constant phase element (CPE) as an active electrochemical element in the model circuit has rather facilitated the study of such inhomogeneous surfaces,[17−19] only a few studies that employed EIS solely have appeared. Contradictory views regarding the nature of partial reactions at copper-electrolyte interface exist. Two models are proposed to explain the growth of passive film; dissolution/precipitation for Cu_2O and CuO and nucleation for CuO.[7]

The present work is an effort to explain the mechanism responsible for the growth of the passive film, mainly comprised of Cu_2O and $CuO/Cu(OH)_2$ and ultimately its breakdown when static potential is varied, in standard buffer solution, pH 9.2, using EIS as the main technique.

Experimental

Copper disc of 1 mm thickness and 1cm diameter was used to prepare the working electrode. Analysis of copper metal used for making disc, as working electrode showed that it contained less than 0.5% impurities (0.03% iron, 0.39% zinc). The disc was fixed on a glass tubing using araldite (Ciba-Giegy). Its thickness was reduced to 0.5 mm by mechanical abrasion over sand papers of various grit sizes, including aluminum oxide (No. 1) and silicon carbide (Nos. 400-1200) papers. Eventually, mirror shine was achieved by buffing the disc with buffing paste. The disc was then immersed in acetone for 30 min to remove sticking paste and particles. Caroic acid (5% H_2O_2 + 10% H_2SO_4) was used to finally remove impurities due to oxidation of metal. The disc was then rinsed with water.

Buffer solution of pH 9.2 was prepared by dissolving buffer tablets from BDH in triply distilled water. Before making electrochemical measurements the working electrode was pre-treated at -1.40 V for 45 s. Cyclic voltammogram was recorded using a 3-electrode configuration, with a spirally coiled platinum wire as the counter electrode and saturated calomel electrode as the reference electrode. All potentials in this work were referred to SCE.
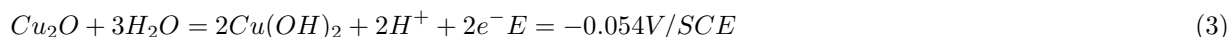
Impedance data in the frequency range of 30 mHz to 100 kHz was collected using the 3-electrode system, on a TFA 2000 Impedance Analyzer from Sycopel Scientific, U.K. The interfering circuit of the reference electrode was removed by connecting a platinum wire electrode serving as sonde via a 10 μF capacitor. The strength of the perturbation potential used in all measurements was 5 mV peak to peak. Prior to measurement at each potential the sample disc was potentiostatically polarized to the desired potential. The impedance data was collected after the waiting period of 10 min.

Results and discussion

Cyclic voltammetric studies

The cyclic voltammogram as in Figure 1 (CV) of the copper disc electrode in a buffer solution of pH 9.2 showed an anodic and 2 cathodic current peaks. According to Pourbaix[1] following equilibriums were expected in the copper/aqueous solution system at pH 9.2.

$$2Cu + H_2O = Cu_2O + 2H^+ + 2e^- \quad E = -0.324V/SCE \tag{1}$$

$$Cu_2O + H_2O = 2CuO + 2H^+ + 2e^- \quad E = -0.114V/SCE \tag{2}$$

$$Cu_2O + 3H_2O = 2Cu(OH)_2 + 2H^+ + 2e^- \quad E = -0.054V/SCE \tag{3}$$

The current peak A_1 was due to the electroformation of Cu_2O barrier layer (Eq. 1) and the anodic formation of a complex hydrous CuO layer (Eqs. 3 and 2), which was overlaid upon the barrier layer and gave a duplex structure to it. The latter layer was responsible for the decrease in anodic dissolution of copper. The 2 cathodic peaks were unquestionably due to electroreduction of CuO and $Cu(OH)_2$ to Cu_2O, and Cu_2O to Cu respectively.[20]
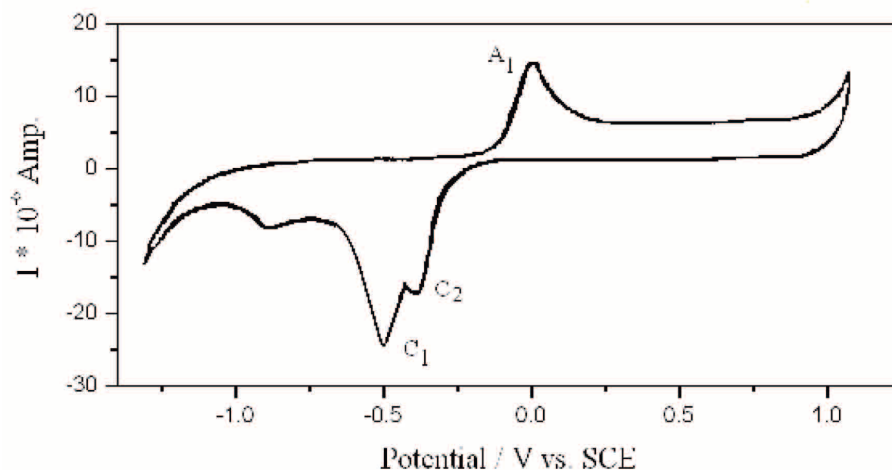

Figure 1. Cyclic voltammogram of copper in buffer solution of pH 9.2 at a scan rate of 50 mV s^{-1}.

The anodic peak appeared broader and dragged in the anodic direction. The appearance of more than one anodic peak in the cyclic voltammogram was pH and sweep rate dependent.[10,16] That only one anodic peak observed was not surprising because of the relatively high scan rate used in this study. Even a scan rate of 20 mV s^{-1} did not resolve anodic peaks.[20] Strehblow and Titze[10] obtained 2 well resolved anodic peaks with a distinct broad shoulder to higher potential peak at 0.1 mV s^{-1} scan rate. However, in the same system (pH 9.2 borate buffer) at 20 mV s^{-1} sweep rate although 2 anodic peaks were observed, the higher potential peak was weaker and dragged. Therefore, the observed anodic peak in the present study is assigned to electroformation of Cu_2O and complex $CuO/Cu(OH)_2$.

Electrochemical impedance spectroscopic studies

The impedance characteristics of the freshly prepared copper disc electrode were measured employing an AC signal of 5 mV amplitude in the frequency range of 30 mHz -100 kHz at 13 static potentials from -0.3 V to 0.9 V. The potential in this range was progressively increased in steps of 0.1 V. The experimental data were analyzed and fitted using equivalent circuits through software by Boukamp,[21] which also made use of some elements as calculation variables.[22]

On the basis of the circuits used to fit the impedance data the entire potential range brought out 3 distinct potential stages: (a) initial stage, -0.3 to 0.1 V (b) middle stage, 0.2 to 0.3 V, and (c) final stage, 0.4 to 0.9 V.

Equilibrium redox potentials for the formation of Cu_2O from copper and CuO, $Cu(OH)_2$ from Cu_2O (Eqs. 1, 2, and 3) showed that in the first potential region the formation and growth of the inner layer of Cu_2O and the outer layer of $CuO/Cu(OH)_2$ overlaying the Cu_2O barrier layer occurred as in Figure 2. Capacitive circuit (inset Figure 3), which characterized a diffusion process represented the behavior of the modified film. In the third potential region diffusion controlled kinetic phenomenon changed to a charge transfer process especially at 0.4 and 0.7 V. In this region CuO oxide layer grew using Cu^{1+} ions from the inner Cu_2O layer and then $Cu(OH)_2$ from CuO at higher potential.
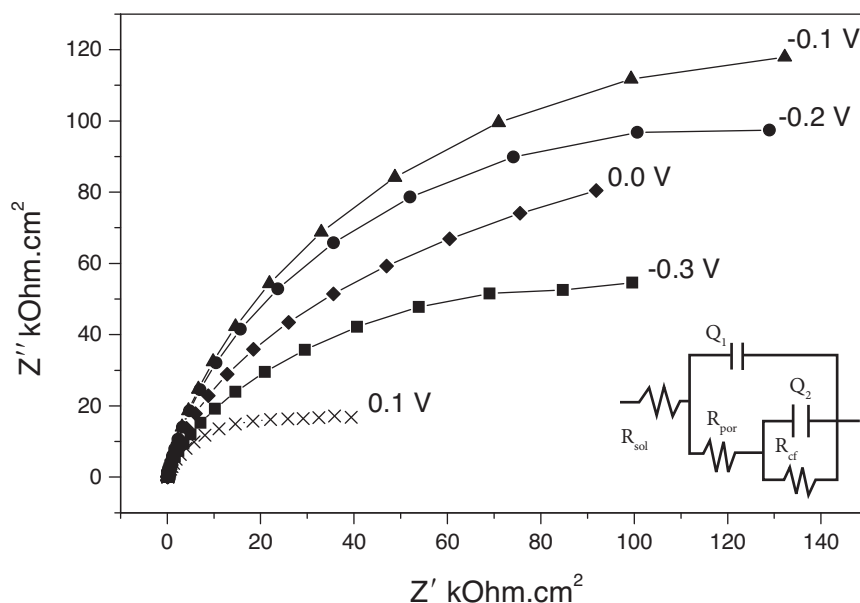

Figure 2. Nyquist plots for the initial stage of passivation of copper surface.

It is to be pointed out that EIS is a potentiostatic technique and prior to EIS measurements at each potential step, the electrode was given sufficient time for stabilization.

(a) Initial Stage

Complex plane plots, Z' vs. Z'', are shown in Figure 2 for potentials of the initial stage. A complete semicircle was not observed; instead a highly reactive arc was obtained, which rose steeply from the higher frequency end. At 0.0 V, structural transformations began in the film and were enhanced at 0.1 V. The Nyquist plot of 0.1 V potential became almost parallel to the Z' axis at low frequencies. The dissolution also affected the homogeneity of the surface leading to incoherent response of different species present to the applied signal.

The behavior of the film in relation to its continuously varying structure on application of potential is best represented by fitting the impedance data (Table) to the circuit in the inset of Figure 2. Better agreement was achieved between theoretical and experimental results by including frequency dependent constant phase elements (CPEs), Q_1 and Q_2 in the circuit. A CPE was introduced instead of pure capacitance and Warburg impedance. In the proposed circuit CPE represented interfacial capacitance Q_1 in parallel with a sub-circuit involving charge transfer resistance (R_{ct}). The circuit represented the characteristics of the underlying Cu_2O layer and the duplex layer.

Table. Best fit parameters of copper surface at various potentials.

Potential in V	$Q_1 * 10^{-6}$ Ω^{-1} cm^{-2} s$^{0.5}$	n_1	R_{por} kΩ cm^2	R_{ct} kΩ cm^2	$Q_2 * 10^{-6}$ Ω^{-1} cm^{-2} s$^{0.5}$	n_2
-0.3	23.7	0.85	0.056	122	4.08	1.00
-0.2	4.74	1.00	0.060	236	11.9	0.84
-0.1	4.82	1.00	0.061	287	11.8	0.84
0.0	5.95	1.00	0.107	193	12.8	0.76
0.1	9.26	0.96	0.257	49	15.2	0.70
0.2	6.74	0.88	5.77	-	42.8	0.35
0.3	4.65	0.89	32.1	-	23.2	0.22
0.4	21.7	0.81	5.23	4.22	109	0.56
0.5	31.5	0.84	10.4	23.2	116	0.76
0.6	25.2	0.86	7.40	43.2	49.6	0.51
0.7	30.2	0.88	7.03	15.3	22.5	0.53
0.8	36.6	0.84	2.61	14.6	50.5	0.56
0.9	49.1	0.82	1.53	17.6	46.1	0.59

In general CPE appeared due to a distribution of relaxation times arising from inhomogeneities present at the microscopic level in the oxide phase and at the oxide/electrolyte interface. The static disorder such as porosity,[23] a random mixture of insulator and conductor described by the effective medium approximations as percolation,[24] an interface that can be described by fractal geometry,[25] an RC transmission line,[26,27] or dynamic disorder, such as diffusion, are contributors to CPE. The impedance of a CPE is defined by Eq. (4).

$$Z_{CPE} = [Q(j\omega)^n]^{-1} \tag{4}$$

When n = 1, Q becomes equivalent to a true capacitance (ideal case of no dispersion); for n = 0, Q becomes equivalent to a resistance. The value of n = 0.5 corresponds to diffusion of a reactant in a Faradaic process and Q becomes equivalent to Warburg impedance. At intermediate values 1 > n > 0.5, Eq. (4) describes frequency behavior of a constant phase element, which contrary to Warburg impedance is not dependent on the presence or absence of redox reactions. Magnitude of the exponent n indicates the extent of surface homogeneity. Poor surface homogeneity is related to some type of pore structure permeating solvent through it.

The electrolyte/film interface was represented by Q_1 and film/metal interface by Q_2. R_{por} and R_{ct} represent film resistance and charge transfer resistance, respectively. Similarly n_1 represents inhomogeneity of the electrolyte/oxide interface and n_2 represents homogeneity of the film/metal interface. The rate of corrosion was controlled by the charge transfer resistance R_{ct} and the undergoing structural changes of the passive layer were indicated by Q_1 and Q_2. The Q_2 and R_{ct} combination characterized a higher time constant and therefore it was connected to the processes occurring at lower frequencies.

The Q_1 and R_{por} parallel combination characterized a lower time constant and it was connected to the processes occurring at higher frequencies. It reflects the properties of the oxide/electrolyte interface. It refers to the double layer capacitance and resistance of electrolyte in the pores of the oxide film. The contribution to

the overall impedance from the porous outer layer with pores filled with electrolyte would be small when the outer layer is thin. In such a case the charge transfer resistance dominated the impedance.

Theoretically, Eqs. (5) and (6) provided the criteria that should be met for the experimental data to be resolved into 2 parts. Each time constant gave rise to a semicircle when the 2 time constants were quite far apart from each other so that the phenomena represented by them were not interacting and these can be studied independently.[28]

$$0.2 < R_{ct}/R_{por} < 5 \tag{5}$$

and

$$0.05 > \tau_{t/}\tau_p > 20 \tag{6}$$

Here τ_t and τ_p stand for time constants at low frequency and high frequency, respectively. Appearance of one semicircle (incomplete) in Nyquist plots of Figure 2 indicated that 2 time constants did not differ from each other widely as required. The Nyquist plots contained information about the solution/film and the film/metal interfaces and apparently it was unlikely that a second semicircle would be observed due to film resistance and capacitance at frequencies greater than 100 kHz. The observed semicircle therefore represented a charge transfer semicircle, although incomplete, which gave information about the rate of corrosion occurring through the passive film. The diameter and the maximum reactance (Z″) at low frequencies gave R_{ct} and Q_2 strictly in accordance with the equivalent circuit model used. The R_{por} and Q_1 strongly influenced the oxide/electrolyte interface.

The shape of a wide open capacitive arc was characteristic of a capacitor charged via CPE or Warburg impedance due to semi infinite diffusion of the charging species.

R_{ct} values were higher than R_{por} and inversely related to exchange current thus it measured the rate of electron transfer reaction. Higher values of R_{ct} in the -0.3 V to 0.1 V potential range indicated the presence of Cu_2O barrier layer with some $CuO/Cu(OH)_2$ formed[8] at later potentials (0.0, 0.1 V) from Cu_2O. Apparently, the film was compact and protective. The capacitance values in this initial potential stage may be rationalized in terms of the charge transfer processes leading to conversion of Cu to Cu^{1+} and Cu^{2+}, and Cu^{1+} to Cu^{2+}. Low capacitance value (Q_2) in this potential stage suggested near perfect oxide covering of metal[29] with cuprous layer. At -0.3 V, the n_2 value corresponds to that of an ideal capacitor indicating coverage of the electrode surface by well organized Cu_2O component of the bulk oxide film. The decrease in n_2 values with increasing applied potential suggested that the film is losing its initial homogeneity due to reactions of Eqs. (2) and (3).

Q_1, n_1, R_{por} parameters characterized the oxide film/electrolyte interface. The Q_1 value first decreased followed by a slight increase. At -0.3 V, Cu_2O is formed and this aspect is reflected in the Q_1, n_1 values. With further development of Cu_2O layer at -0.2 and -0.1 V potentials, the interface became more organized and homogenous with the removal of dislocations, edges present. Changes in the interface structure start taking place at 0.0 V and continues at +0.1 V as reflected by corresponding Q_1, n_1. At this potential, copper also dissolved in the form of $HCuO_2^-$ species in buffer of pH 9.2.[10] Such low values of Q_1 suggested negligible contribution of charging current as also noticed in the case of chromium.[30] This trend together with low values of R_{por} suggested that the outer layer is thin with pores filled with little electrolyte.

Middle stage

Best fit Nyquist plots are shown in Figure 3 for 0.2 and 0.3 V. An incomplete circle at high frequencies interacted with a "reactive tail" at low frequencies at an angle of $45°$ with the Z' axis. The shape was characteristic of a diffusion controlled process, which in this case was responsible for the movement of ions and accumulation of charge in the bulk film. At 0.3 V, the Nyquist plot is a circular arc at the high frequency side which changed to an arched line at low frequencies indicating the presence of a CPE. Both impedance (Z', Z'') values have increased as compared to that at 0.2 V potential indicating more compactness and rigidity of the film by diffusion of ionic species into the duplex layer.
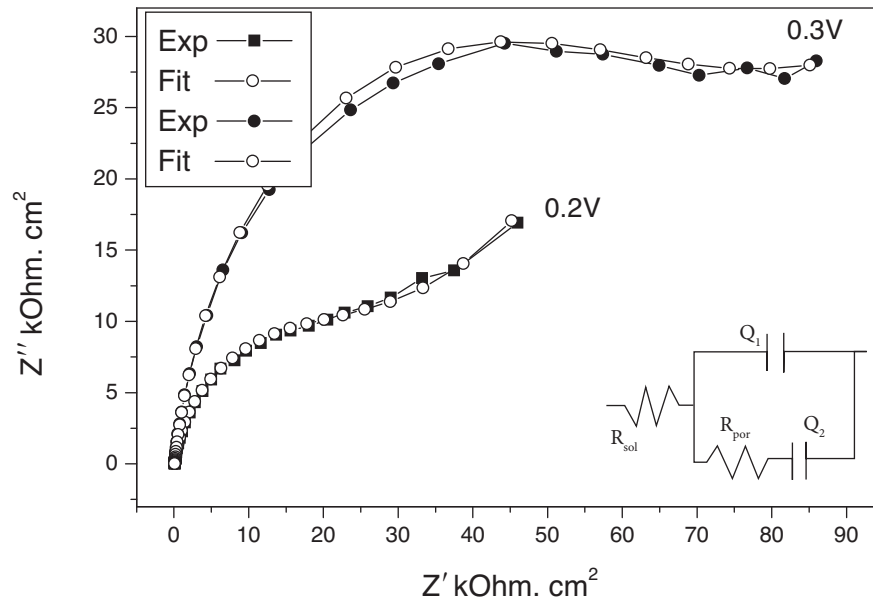

Figure 3. Nyquist plots for the second stage of passivation of copper surface.

The proposed circuit (inset of Figure 3) represented diffusive character of the film. It consisted of an electrolyte/film interface denoted by Q_1 in parallel with R_{por} (film resistance) and another for film/metal interface Q_2. Kinetic parameter, diffusion coefficient was calculated using the following equation:[31]

$$S = RT/n^2F^2c\sqrt{2D}; S = 1/(Q_2\sqrt{2}) \tag{7}$$

The diffusion coefficient value is of the order of $10^{-9}\,cm^2\,s^{-1}$ and suggested a protective film where ion movement was low and potential dependent. According to point defect model the oxidation of metal atoms to form ions at the metal/oxide (inner) interface generated a driving force to form anion vacancies.[32,33]

$$Cu_{Cu}(m) = Cu_{Cu}(ox) + 1/2V_o^{··}(ox) + e \tag{8}$$

where $Cu_{Cu}(m)$, a copper atom in a regular metal site, $Cu_{Cu}(ox)$, a copper cation in a regular site of the oxide film, $V_o^{··}$, a positively charged oxygen vacancy, and e represented the electron. At the oxide/electrolyte (outer) interface anion vacancies became occupied by anions:

$$V^{··}o(ox) + H_2O(aq) = O_o(ox) + 2H^+(aq) \tag{9}$$

745

where $O_o(ox)$, an oxygen anion in a regular site of the oxide film and H^+(aq), the hydrogen ion in the aqueous electrolyte. Cation vacancies, which were formed by dissolution of cations into the electrolyte diffused towards the inner interface:

$$Cu_{Cu}(ox) = Cu^+(aq) + V'_{Cu}(ox) \qquad (10)$$

where these could be exchanged with cations:

$$Cu_{Cu}(m) + V'_{Cu}(m) = Cu_{Cu}(ox) + V_{Cu}(m) + e \qquad (11)$$

Cu^+(aq), a positively charged copper cation in the aqueous electrolyte, V'_{Cu}(ox), a negatively charged cation vacancy in the oxide, and V_{Cu}(m), a neutral vacancy in a regular metal site.[34]

$$Cu_{Cu}(ox) = Cu^+_{\text{duplex}} + V''_{Cu(ox)} \qquad (12)$$

where Cu^+_{duplex} showed the ion that moved into the duplex film and $V''_{Cu(ox)}$, vacancy created in the Cu_2O layer.[35]

The interfacial capacitance (Q_1) of the oxide/electrolyte interface slightly decreased on increase in potential. However, constant n_1 values showed that the interfacial homogeneity is retained. The Q_1 values are typical capacitance values observed for an oxide covered surface of metal.[29] An increase in R_{por} at 0.2 V and then further to a maximum value at 0.3 V suggested that the Cu^{1+} ions from the inner Cu_2O layer diffuse and accumulated in the duplex layer. In this buffer solution, 0.2 V and 0.3 V are those applied potentials, where compressive stress developed in the crystals causing ejection of Cu^{1+} ions into the duplex film.[36] For the same reason Q_2 increased but n_2 decreased. The small n_2 values were characteristic of the solid electrolyte[37] and electrochemical systems.[34,38] The increased resistance caused blocking of the percolation of the molecules into the passive film although the film appeared to be amorphous in nature (low n_2 value) and behaves like solid electrolyte[37].

Final stage

Best fit Nyquist plots in Figure 4 for the 0.4 V – 0.9 V potentials range showed a skewed semicircle at 0.4 V. At this potential a charge transfer process owing to the presence of Cu^{1+} occurred that resulted in the CuO growth.

At 0.5 and 0.6 V the skewed semicircle transformed into a rising curve, almost linear at the low frequency end suggesting diffusion of OH^- opposite to Cu^{1+} due to increased porosity.

The change of Nyquist plots along with Z' and Z'' suggested that the charge transfer process appeared to have slowed down considerably and the diffusion process took over. At 0.7 V again a skewed semicircle appeared which gradually opened up as the potential increased to 0.9 V. Corresponding Z' and Z'' values for the peaks were respectively 4.2 and 2.7 kΩ cm^2 for 0.4 V and 7.6 and 4.8 kΩ cm^2 for 0.7 V. The maxima in the skewed semicircles in the Nyquist plots for 0.4 V and 0.7 V were observed at 1.08 Hz and 294 mHz, respectively. The increase in the Z' values at these potentials may be correlated with the molar volume increase on transformation of underlying Cu_2O to CuO and $Cu(OH)_2$ at oxide/metal interface due to diffusion. Formation of $Cu(OH)_2$ is expected at 0.7 V since thermodynamically this compound is formed at a higher potential.[1,8] w
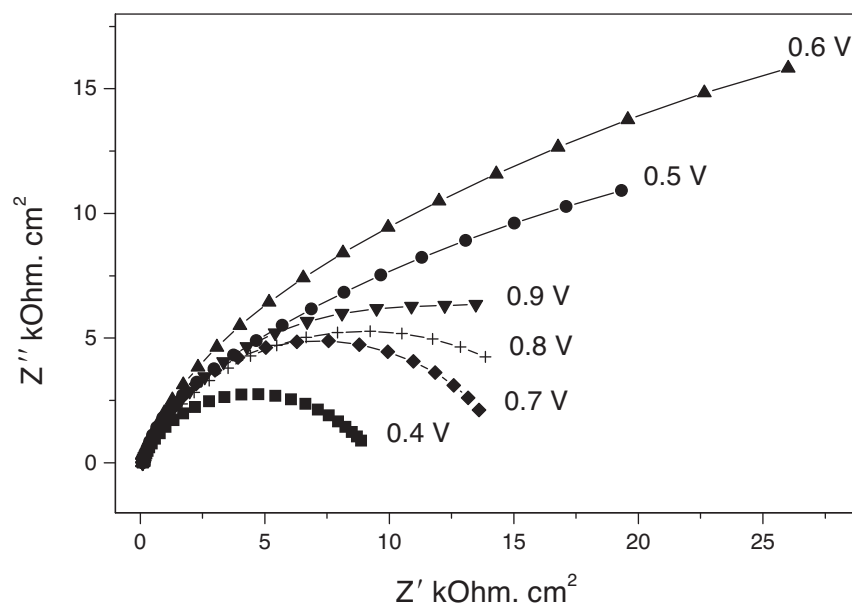
Figure 4. Nyquist plots for the final stage of passive copper surface.

At 0.8 V, the semicircle structure of the plot is still retained, but the maximum now shifted further to a lower frequency (212 Hz). At this potential it is assumed that formation of hydroxide still continued leading to change in the structure of the oxide/electrolyte interface. At 0.9 V, the shape of the Nyquist plot changed toward the low frequency end. The maximum may be located somewhere near 30 mHz. Apparently, potential increase modified the amorphous structure of the film. First, film thickness increased with the formation of CuO from Cu_2O, and later conversion to $Cu(OH)_2$ produced wide pores in the film, eventually, facilitated the movement of ions from solution to metal surface. Passivity of the film was thus broken down, i.e. trans-passive region was reached with filling of pores with solution. Aluminum oxide films were also porous when formed but they possessed a barrier type layer underneath.[19,20] In case of copper the increased potential destroyed the passive film.

The influence of potential change on the metal/oxide and oxide/electrolyte interfaces was reflected in the values of the best fit parameters also. The growth of the duplex film was accompanied by the formation of CuO, which restarted at 0.4 V after diffusion of Cu^{1+} stopped into the duplex film. The formation of CuO islands from the oxidation of Cu_2O increased the roughness of the surface[39] as also shown in the scanning tunneling microscopy (STM).[40] The resistance R_{por} increased and attained a maximum value of $10.4 \, k\Omega \, cm^2$ at 0.5 V due to CuO growth on the electrode surface which had a smaller molar volume ($12.4 \, cm^3 \, mol^{-1}$) than Cu_2O ($23.9 \, cm^3 \, mol^{-1}$), thus made the film compact. Simultaneously, Q_1 and n_1 values increased. With further increase in potential, both the R_{por} and Q_1 decreased, which may be due to the variation in the film texture. At 0.7 V conversion of CuO to $Cu(OH)_2$ through a charge transfer process slightly decreased R_{por} and increased Q_1 and n_1, indicating trapping of charged species, due to the dissolution of $Cu(OH)_2$ having molar volume of $29.0 \, cm^3 \, mol^{-1}$.

The charge transfer process continued at 0.8 V and 0.9 V also causing further decrease in R_{por} and increase in Q_1. Dissolution of $Cu(OH)_2$ may also be a factor at these potentials that affected the value of n_1.

According to the band structure model of semiconductors, crossing of valence band and fermi level above 0.308 V for Cu_2O inject an acceptor level, i.e. Cu^{2+} states, which finally leads to the formation of CuO and $Cu(OH)_2$ as the potential increased to 0.708 V. According to Strehblow, any further potential increase would be located in the Cu(II) oxide/electrolyte interface.[9] Therefore, it is expected that potential increase to 0.7 V would give hydroxide of copper according to the reaction:[41]

$$CuO + 2OH^- \rightleftarrows Cu(OH)_2 + O^{2-} \tag{13}$$

The Q_2 values together with n_2 values reflected the potential dependence of the film structure.

Nyquist plot analysis at 30 mHz

The Z′ and Z″ values at 30 mHz are plotted in Figure 5. In the initial stage of formation, high resistance and low capacitance values indicated the growth of protective passive film where minimum charge separation is observed. This is followed by another peak in the middle region of film formation. The low Z′ value in this region shows structural changes accompanied with slightly increased capacitance values. Lowest values of Z′ are observed in the 0.4 V to 0.9 V potential region while the maximum charge separation took place at 0.4 V in the film. Additionally, 0.7 V is another potential value where charge separation was observed. These variations clearly indicated the structural changes in the film as potential move anodic.
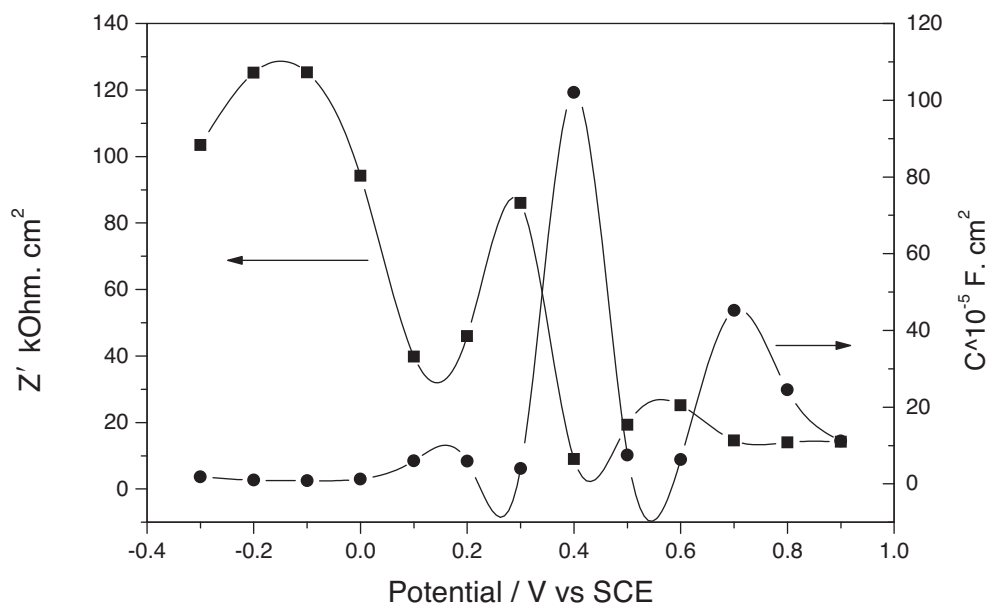

Figure 5. Variation of Z′ and capacitance (C) with potential at 0.03 Hz.

Conclusion

The corrosion process strongly depended upon the applied potential. In the first potential stage, the film was the most stable and its formation and growth over the polycrystalline copper surface followed a consistent pattern in the negative potential regime.

The second stage acted like the demarcation line between passivation and trans-passivation stages. Diffusion coefficient calculated in conjunction with impedance spectra showed that film was protective with difficult ion movement.

In the final potential stage the film structure was severely affected by increasing potential. So electrolyte supersaturated with Cu^{2+} ions adjacent to the metal surface did not cause precipitation of oxides rather direct oxide growth seems very likely.

References

1. Pourbaix, M. In *Atlas of the Electrochemical Equilibria in Aqueous Solution*; Chap. 4, pp. 384-392, Pregmon Press, New York, **1966**.

2. Y. Feng, W. K. Teo, K. S. Siow, G. L. Tan, A. K. Hsieh. Corros. Sci. **1996**, 38, 369-387.

3. Feng, Y.; Siow, K. S.; Teo,W. K.; Tan, K. L.; and Hseih, A. K. *Corrosion (Houston),* **1997**, 53, 389-398.

4. Kautek, W.; and Gordon II, J. G. *J. Electochem. Soc.,* **1990**, 137**,** 2672-2677.

5. Halliday. J. S. *Trans. Faraday Soc.* **1954**, 50, 171-178.

6. Hickling A.; Taylor. D. *Trans. Faraday Soc.* **1948**, 44, 262-268.

7. Dignam, M. J.; and Gibbs, D. B. *Can. J. Chem*. **1970**, 48, 1242-1250.

8. Shoesmith, D. W.; Rummery, T. E.; Owen, D.; Lee, W. *J. Electrochem. Soc.* **1976**, 123, 790-799.

9. Strehblow,H.-H.; Collisi. U.; Druska, P. *International Symposium on Control of Copper Alloys Oxidation,* **1992**, *Rouen,* Tranrvied, 6.-8. 7.

10. Strehblow, H.-H.; Titze, B. *Electrochim. Acta.* **1980**, 25, 839-850.

11. Strehblow, H.-H.; Maurice, V.; Marcus. P. *Electrochim. Acta.* **2001**, 46, 3755-3766.

12. Ambrose, J.; Barradas, R. G.; Shoesmith, D. W. *J. Electroanal. Chem.* **1973**, 47, 47-64.

13. Droog, J. M. M.; Alderliesten, C. A.; Anderliesten, P. T.; Bootsma G. A. *Electroanal. Chem.*. **1980,** 111, 61-70.

14. Diard, J.-P.; Le Canut, J.-M.; Le Gorrec, B.; Montell. C. *Electrochim. Acta.* **1998**, 43, 2469-2483.

15. Diard, J.-P.; Le Canut, J.-M.; Le Gorrec, B.; Montell.C. *Electrochim Acta.* **1998**, 43, 2485-2501.

16. Babic, R.; Metikos-Hukovic, M.; Jukie, A. *J. Electrochem. Soc.* **2001**, 148, B146-B151.

17. Juttner, K.; *Electrochim Acta*, **1990**, 35, 1501-1508.

18. Hitzig, J.; Juttner, K.; Lorenz, W. J.; Paatsch, W. *Corrosion science***, 1984**, 24, 11/12, 945-952.

19. Hitzig, J.; Juttner, K.; Lorenz, W. J.; Paatsch, W. *J. Electrochem. Soc.***, 1986**, 133 (5), 887-892.

20. Milosev, I.; Metikos- Hukovic, M. *Electrochim Acta***, 1997**, 42, 1537-1548.

21. Boukamp, B. A. *EQUIVCRT software manual,* University of Twente Enschede, The Netherlands, 1993.

22. Gabrielli, C. *Identification of Electrochemical Processes by Frequency Response Analysis,* Technical report number 004/83, Solartron Instruments, England.

23. Kramer, M.; Tomkiewicz, M. *J. Electrochem. Soc.* **1984**, 131, 1283-1288.

24. Tomkiewicz,M.; Aurian-Blajeni, B. *J. Electrochem. Soc.* **1988**, 135**,** 2743-2747.

25. Lin, H. S. *Phys. Rev. Lett. **1985***, 55, 529-532.

26. Macdonald, J. R. *Solid State Ionics**. **1984***, 13, 147-149.

27. Omanovic, S.; Metikos-Hukovic, M. *Thin Solid Films.* **1995**, 266, 31-37.

28. Walter, G. W. *J. Electroanal. Chem.* **1981**, 118, 259-273.

29. Fernandes J. C. S.; Ferreira, M. G. S.; Rangel, C. M. *J. Appl. Electrochem**. **1990***, 20**,** 874-876.

30. Moffat, T. P.; Latanision**,** R. M. *J. Electrochem. Soc.* **1992**, 139, 1869-1879.

31. Metikos-Hukovic, M. ; Omanovic, S. *J. Electroanal. Chem**. **1998***, 455, 181-189.

32. Chao, C. Y.; Lin, L. F.; Macdonald, D. D. *J. Electrochem. Soc.* **1981**, 128, 1187-1194.

33. Macdonald, D. D.; Ben-Haim M.; Pallix, J. *J. Electrochem. Soc.* **1989**, 136**,** 3269-3273.

34. Raistrick, I. D.; Ho, C.; Huggins, R. A. *J. Electrochem. Soc.* **1976**, 123, 1469-1476.

35. Young, L. *J. Electrochem. Soc.* **1963**, 110, 589.

36. Vermilyea, D. A. *J. Electrochem. Soc.* **1963**, 110, 345-346.

37. Tsai, Y. T.; Whitemore, D. H. *Solid state ionics**. **1982***, 7**,** 129-139.

38. Bottelberghs P. H.; Broers, G. H. J. *J. Electroanal. Chem**. **1976***, 67**,** 155-167.

39. Collisi Udo; Strehblow, H-H. *J. Electroanal. Chem**. **1990***, 284**,** 385-401.

40. Maurice, V.; Strehblow H.-H.; Marcus, P. *J. Electrochem. Soc.* **1999,** 146, 524-530.

41. Lohrengel, M. M.; Schultze, J. W.; Spekmann, H. D.; Strehblow, H.-H. *Electrochim. Acta**, **1987***, 32, 733-742.